

$$R_3 = \bar{\Delta}^2 [\rho_4 (A_1 \gamma_+ + A_1 \omega \beta_- - 2\bar{B}_1 \gamma_+) - D_2 \{ A_1 (3\rho_1 + 6\beta_+ - \omega \rho_3) - 2\bar{B}_1 (3\gamma_+ - \rho_3) \}] / 4P, \quad (\text{A16c})$$

$$R_4 = \bar{\Delta} [\rho_4 \{ A_1 \beta_+ \rho_1 - 2\bar{B}_1 (\gamma_+ + \omega \beta_-) \} - D_2 \{ A_1 \rho_1 (3\beta_+ + \rho_3 P^2) - 2\bar{B}_1 (3\rho_1 + 6\beta_+ - \omega \rho_3) \}] / 4P, \quad (\text{A16d})$$

$$R_5 = \bar{B}_1 [-\rho_4 \beta_+ \rho_1 + D_2 \rho_1 (3\beta_+ + \rho_3 P^2)] / 2P, \quad (\text{A16e})$$

$$R_6 = A_1 \bar{\Sigma}^2 [\rho_4 \beta_+ - D_2 (3\beta_+ + \rho_3)] / 8P\omega, \quad (\text{A16f})$$

$$R_7 = -2\bar{B}_1 R_6 / A_1 \bar{\Delta}. \quad (\text{A16g})$$

To complete the analysis we must evaluate the fundamental integrals (A9), (A10), and (A14). Although this cannot be done in closed form, rapidly converging series expansions are obtainable using the same method

as employed in I. We observe that all the fundamental integrals are of the form

$$F_n = \int_0^1 dx x^{-\eta} (1-x)^{\eta} f_n(x). \quad (\text{A17})$$

Detailed examination reveals that the $f_n(x)$ are relatively slowly varying functions over the interval $0 \leq x \leq 1$ for all cases. The structure of the integrand then suggests that, if $f_n(x)$ is expanded in a Maclaurin series, the resulting series for F_n will converge quite rapidly. Performing such an expansion, we obtain

$$F_n = n! \sum_{k=0}^{\infty} \frac{f_n^{(k)}(0)}{k!(1+k-\eta)(2+k-\eta)\cdots(n+1+k-\eta)}, \quad (\text{A18})$$

from which the various fundamental integrals may then be evaluated.

Triton Reactions near 2 MeV: Elastic Scattering

G. H. HERLING,* L. COHEN, AND J. D. SILVERSTEIN†

Naval Research Laboratory, Washington, D. C. 20390

(Received 19 August 1968)

Tritons have been elastically scattered from a number of light nuclei, and the data have been analyzed in terms of the optical model. Geometries have been found which are applicable to ${}^9\text{Be}$, ${}^{10,11}\text{B}$, and ${}^{12}\text{C}$, and to ${}^{19}\text{F}$ and ${}^{20}\text{Ne}$. The real central well depths are approximately 140 MeV, and the spin-orbit well depth is greater than that expected from theoretical considerations. Ambiguities in the parameters are discussed.

1. INTRODUCTION

THERE has recently been much interest in the scattering and reactions induced by mass-three particles. Because of the success in describing the elastic scattering of deuterons and α particles with the optical model, a similar analysis for the scattering of ${}^3\text{H}$ appears plausible. Many optical-model analyses of ${}^3\text{He}$ scattering have been performed,¹ but there have been relatively few analyses for tritons.²⁻⁸ The present paper is concerned with an optical-model analysis of the elastic

scattering of tritons with bombarding energies near 2 MeV.

Although the triton energy is low, the scattering from the target nuclei ${}^9\text{Be}$, ${}^{10}\text{B}$, ${}^{11}\text{B}$, ${}^{12}\text{C}$, ${}^{19}\text{F}$, and ${}^{20}\text{Ne}$ generally exhibits structure that is capable of yielding optical-model parameters which may be further tested by their employment in distorted-wave Born approximation (DWBA) calculations. In order to reduce the region of the parameter space searched, the results of other analyses have been used to obtain starting points for the calculations. Additional constraints on the acceptable solutions are supplied by the theoretical model, which suggests that the optical potential for a complex projectile should be the sum of the nucleon optical potentials for its constituents averaged over their internal wave function.⁹⁻¹²

In Secs. 2 and 3 the triton experiments and optical-model analysis are briefly considered. In Sec. 4 there

* Present address: State University of New York, Stony Brook, N.Y. On leave from the Naval Research Laboratory.

† National Research Council, U.S. Naval Research Laboratory Postdoctoral Resident Research Associate.

¹ P. E. Hodgson, Institute of Physical and Chemical Research Cyclotron Progress Report Suppl. 1, 1968, p. 41 (unpublished).

² D. J. Pullen, J. R. Rook, and R. Middleton, Nucl. Phys. 51, 88 (1964).

³ J. H. Bjeregaard, H. R. Blieden, O. Hansen, G. Sidenius, and G. R. Satchler, Phys. Rev. 136, B1348 (1964).

⁴ J. R. Rook, Nucl. Phys. 61, 219 (1965).

⁵ R. N. Glover and A. D. W. Jones, Phys. Letters 16, 69 (1965).

⁶ R. N. Glover and A. D. W. Jones, Nucl. Phys. 81, 268 (1966).

⁷ A. G. Blair and D. D. Armstrong, Phys. Rev. 151, 930 (1966).

⁸ J. C. Hafele, E. R. Flynn, and A. G. Blair, Phys. Rev. 155, 1238 (1967).

⁹ S. Watanabe, Nucl. Phys. 8, 484 (1958).

¹⁰ J. L. Gammel, B. J. Hill, and R. M. Thaler, Helv. Phys. Acta Suppl. 6, 409 (1961).

¹¹ A. Y. Abul-Magd and M. El-Nadi, Progr. Theoret. Phys. (Kyoto) 35, 798 (1966).

¹² L. R. Veaser, D. D. Armstrong, and P. W. Keaton, Jr., Bull. Am. Phys. Soc. Ser. II, 13, 117 (1968).

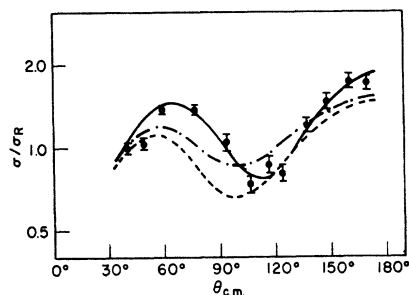


FIG. 1. Fits obtained to 2.0-MeV tritons elastically scattered from ${}^9\text{Be}$ for three different starting points. The dashed curve is based upon Ref. 7; the dot-dash curve is based upon Ref. 21; the solid curve is the best fit.

are further details about the analysis, and the results of the calculations are discussed.

2. EXPERIMENTS

Tritons from the Naval Research Laboratory 2 MV Van de Graaff accelerator were magnetically analyzed and directed into a 26.7-cm-i.d. scattering chamber equipped with fixed ports covering the range from 15° to 165° in $7\frac{1}{2}^\circ$ intervals. The chamber was equipped with a top containing a rotating turret which allowed the selection of any one of six target foils; it could also be employed for differentially pumped gaseous targets. The scattered tritons were detected with silicon surface-barrier detectors.

Absolute differential cross sections were measured for ${}^9\text{Be}$ by employing as a monitor the elastic scattering from a thin layer of gold flashed onto the target.¹³ The ${}^{10}\text{B}$ data were obtained from isotopically enriched (approximately 98%) self-supporting foils. Both the experiment and the differential cross section are given in a previous publication.¹⁴ Similarly, the ${}^{11}\text{B}$ data were obtained from 98% isotopically enriched self-supporting foils, and the cross section arbitrarily set to the Rutherford value at the smallest angle of observation.¹⁵ The ${}^{12}\text{C}$ data were also normalized to the Rutherford cross section at the forward angles.¹⁶ It is believed that the

TABLE I. Triton optical-model parameters for p -shell nuclei. $r_0 = 0.85$ fm; $a = 0.704$ fm; $r_0' = 2.06$ fm; $a' = 0.722$ fm; $r_C = 1.40$ fm.

Target	${}^9\text{Be}$	${}^{10}\text{B}$	${}^{11}\text{B}$	${}^{11}\text{B}$	${}^{12}\text{C}$
E_t (MeV)	2.10	1.50	1.75	2.10	1.50
V (MeV)	145	138	138	145	120
W (MeV)	1.91	3.98	1.94	3.78	1.01
V_{so} (MeV)	8.93	8.10	8.92	8.26	8.56

¹³ L. Cohen and G. H. Herling (unpublished).

¹⁴ H. D. Holmgren, L. M. Cameron, and R. L. Johnston, Nucl. Phys. **48**, 1 (1963).

¹⁵ J. D. Silverstein and G. H. Herling (unpublished).

¹⁶ G. D. Gutsche, H. D. Holmgren, L. M. Cameron, and R. L. Johnston, Phys. Rev. **125**, 648 (1962).

TABLE II. Triton optical-model parameters for (s, d) -shell nuclei. $r_0 = 0.99$ fm; $a = 0.829$ fm; $r_0' = 1.81$ fm; $a' = 0.592$ fm; $r_C = 1.40$ fm.

Target	${}^{19}\text{F}$	${}^{20}\text{Ne}$
E_t (MeV)	2.00, 1.80	2.00, 1.90
V (MeV)	150	150
W (MeV)	16	16
V_{so} (MeV)	0	0

normalization of the boron and carbon data has an uncertainty of approximately 10%.

The ${}^{19}\text{F}$ data were obtained from CaF_2 targets in which the calcium served as a monitor for the determination of absolute differential cross sections.¹⁷ The cross sections for ${}^{20}\text{Ne}$ were determined by measuring the scattering from a natural neon gas target, which was assumed to be pure ${}^{20}\text{Ne}$, and normalizing to the scattering at 1 MeV, which was assumed to be pure Rutherford.¹⁸

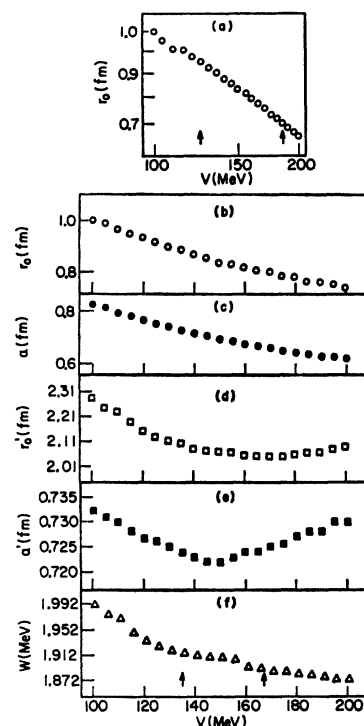


FIG. 2. Ambiguities in the ${}^9\text{Be}$ optical potential. (a) The Vr_0 ambiguity. (b)-(f) The five-dimensional ambiguity. The arrows denote the limits between which χ^2 varies by no more than 30% of its minimum value.

¹⁷ L. M. Cameron, A. R. Knudson, L. Cohen, and G. H. Herling, in *Proceedings of the International Conference on Nuclear Physics, Gallatinburg, Tenn., 1966*, edited by R. L. Becker, C. D. Goodman, P. H. Stelson, and A. Zucker (Academic Press Inc., New York, 1967), p. 171.

¹⁸ L. Cohen and G. H. Herling (unpublished).

Further experimental details will be published elsewhere in reports on one- and two-nucleon transfer reactions.^{13,15,17,18}

3. OPTICAL-MODEL ANALYSIS

The form of the optical potential employed was

$$U = -Vf(x) - iWf(x') - V_{so}\lambda_r^2 \mathbf{l} \cdot \mathbf{s} |r^{-1}(d/dr)f(x)| + V_C, \quad (1)$$

where

$$f(x) = (1 + e^x)^{-1},$$

$$x = (r - r_0 A^{1/3})/a,$$

$$x' = (r - r_0' A^{1/3})/a',$$

and λ_r is the pion reduced Compton wavelength; the orbital angular momentum of a partial wave, in units of \hbar , is l , and \mathbf{s} is related to the triton spin \mathbf{s} by $\mathbf{s} = 2\mathbf{s}/\hbar$. The quantity V_C is the Coulomb potential due to a uniformly charged sphere of radius $r_0 A^{1/3}$. The search

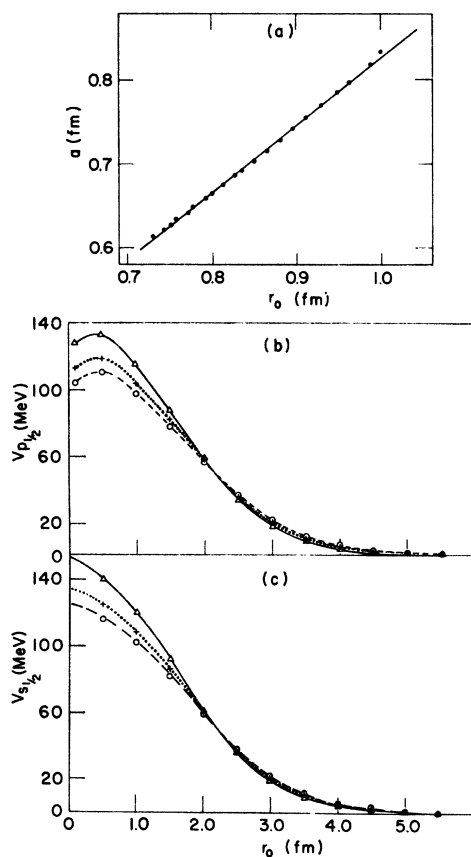


FIG. 3. (a) The (V, r_0, a) ambiguity. (b) Real potential in the $p_{1/2}$ partial wave. (c) Real potential in the $s_{1/2}$ partial wave. The Coulomb potential has been subtracted from the curves shown. The solid curves correspond to $V=165$ MeV, the dotted to $V=145$ MeV, and the dashed to $V=135$ MeV.

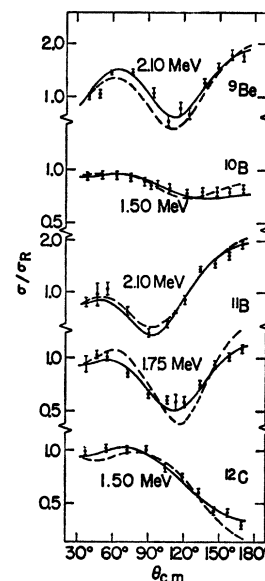


FIG. 4. Optical-model fits to triton elastic scattering from p -shell nuclei. The ^{10}B data are from Ref. 14, the ^{12}C data from Ref. 16. The solid curves are obtained with the parameters of Table I; the dashed curves have the same geometry, but $V_{so} = 2.0$ MeV.

code ABACUS¹⁹ was used to minimize

$$\chi^2 = (1/N) \sum_i [(\sigma_{ti} - B\sigma_{xi})/\Delta\sigma_i]^2, \quad (2)$$

where N is the number of data points in the angular distribution. The theoretical and experimental cross sections at the angle θ_i are denoted by σ_{ti} and σ_{xi} , respectively, while $\Delta\sigma_i$ is the uncertainty in the observation at θ_i . The symbol B refers to possible renormalization of the experimental data.

The uncertainties were chosen to be the statistical errors of the measurements except in the cases of ^{10}B and ^{12}C , for which arbitrary errors of 5% were assigned to all points. The uncertainty in the normalization of the ^{10}B , ^{11}B , and ^{12}C data was taken into account by allowing B to vary between the limits 1 ± 0.15 . It was not, however, optimized by the search code. If a parameter set yielded an acceptable shape for the angular distribution with $B=1$, but disagreed with the normalization of the data, the value of B was changed in order to obtain agreement of the forward-angle cross section. The optical-model parameters were then readjusted in a new minimization of χ^2 . The data for the other targets have not been renormalized.

4. RESULTS AND DISCUSSION

A. Analysis for ^9Be

The ^9Be nucleus presents the lowest Coulomb barrier of those target nuclei considered, and therefore was afforded a central role in the analysis. Several starting points were initially selected in attempting to fit these data.

One set was that obtained in the scattering of 15-MeV tritons from nickel.⁷ The potential obtained for nickel

¹⁹ E. H. Auerbach (unpublished).

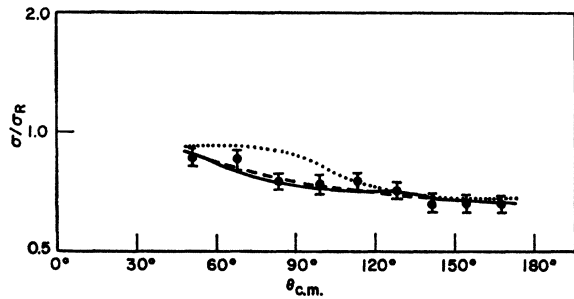


FIG. 5. Fits obtained to 2.0-MeV tritons elastically scattered from ^{19}F . The dotted curve is based upon the p -shell geometry of this work. The dashed curve is a four-parameter fit based upon Ref. 7. The solid curve is based upon Ref. 20 and Eq. (3) of the text.

had $r_0=1.24$ fm and did not include a spin-orbit term.⁷ Only the well depths were initially allowed to vary in the search procedure, but upon being unable to obtain a satisfactory fit, the geometrical parameters were also released. The results are shown as the dashed curve in Fig. 1. Although the calculations do not reproduce the data, the bombarding energy and target mass are so far removed from those considered here that the result is not entirely unexpected.

Other starting points with values of r_0 between 1.0 and 1.4 fm included four-parameter potentials^{5,7} and six-parameter potentials.²⁰ These had real well depths of the order of 150 MeV and imaginary well depths in the region 15–20 MeV. Potentials which produced as much forward scattering as the observations were not obtained from such starting points.

A somewhat improved fit was obtained by choosing as a starting point the parameter set obtained in an analysis of $^3\text{He}+^{13}\text{C}$ elastic scattering.²¹ This set had $r_0=0.93$ fm, and included a spin-orbit term. As before, the geometrical parameters were initially held fixed but were later released in order to find an optimum solution. These results, which are shown as the dot-dash curve in Fig. 1, also misplace the maximum and minimum of the data, and fail to yield as much forward scattering as the observations.

An additional enhancement of the forward scattering could be obtained by further reducing r_0 . The arbitrariness in the reduction could be eliminated, and a correlation with the ^3He potential maintained by employing the relation²²

$$r_0 = R_0 + r_p/A^{1/3}, \quad (3)$$

in which R_0 is assumed to be characteristic of the target shell and r_p of the projectile. Employing the ^3He value²¹ of r_0 and the electron scattering radii²³ of ^3He and ^3H

leads to the value $r_0=0.85$ fm for ^3H , which was then held constant throughout the remainder of the calculations. The use of relation (3) and electron scattering radii is, of course, only to be considered a heuristic device for constraining an otherwise arbitrary parameter change which leads to a fit to the data. The remaining six parameters were then adjusted in order to obtain the fit shown as the solid curve in Fig. 1, and the final values of the parameters are contained in Table I.

Continuous ambiguities in the optical-model parameters were explored for ^9Be . In Fig. 2(a) is plotted the result of calculations for the Vr_0^n ambiguity. The arrows in the figure indicate the limits between which χ^2 varies by not more than 30% of its minimum value. In Figs. 2(b)–2(f), where the arrows have the same meaning as before, are plotted the results of incrementing V in 5-MeV intervals while allowing the imaginary well depth and all geometrical parameters to vary. The imaginary part of the potential is seen to be better determined than the real part. In Fig. 3(a) the values of r_0 and a obtained in these searches are seen to have a linear relation to each other. A similar ambiguity with a negative slope has been reported²⁴ for deuterons, but this work did not include a spin-orbit term in the potential. Because the form factor of the spin-orbit potential contains a derivative with respect to r rather than x , a variation in a changes not only the shape of the potential but also the effective depth. In the present case, the values of V , r_0 , and a generated within the range of the ambiguity are such that for distances greater than about 2 fm the real potentials are nearly equal, as illustrated in Figs. 3(b) and 3(c). This distance is approximately k^{-1} , where k is the reduced wave number of the tritons. Partial waves with $l > 1$ do not contribute appreciably to the cross section.

B. Results for Other p -Shell Nuclei

In fitting the data for ^{10}B , ^{11}B , and ^{12}C , the geometry obtained for ^9Be was held constant and only the well depths were allowed to vary. In all cases the starting

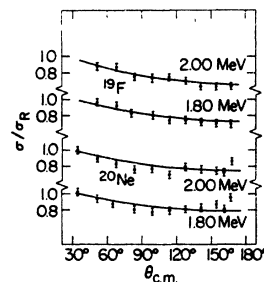


FIG. 6. Optical-model fits to the elastic scattering from (s, d) -shell nuclei. The ^{19}F data are from Ref. 17. The solid curves were obtained with the parameters of Table II, and there is no visible effect of the spin-orbit potential.

²⁰ G. M. Matous, G. H. Herling, and E. A. Wolicki, Phys. Rev. **152**, 908 (1966).

²¹ E. M. Kellogg and R. W. Zurmühle, Phys. Rev. **152**, 890 (1966).

²² G. R. Satchler, Nucl. Phys. **70**, 177 (1965).

²³ H. Collard, R. Hofstadter, E. B. Hughes, A. Johansson, M. R. Yearian, R. B. Day, and R. T. Wagner, Phys. Rev. **138**, B57 (1965).

²⁴ G. S. Mani and F. Picard, in *Comptes Rendus du Congrès International de Physique Nucléaire, II*, edited by P. Gungenberg (Centre National de la Recherche Scientifique, Paris, 1964), p. 902.

point was the parameter set which yielded the best fit for ${}^9\text{Be}$. The best fits for all of the p -shell nuclei are shown in Fig. 4 as solid curves, and the corresponding parameters are contained in Table I. The real well depths are approximately three times the well depth for single nucleons as suggested by the theoretical model.⁹⁻¹² Similarly, the real radius is smaller than that for nucleons and the diffuseness is larger, in qualitative agreement with that model. The imaginary part of the potential is small, which may be due to the fact that fewer channels are open at the low energy considered here. The imaginary radius is smaller than that obtained in Ref. 21, which is in agreement with expectation based upon relation (3).

The depth of the spin-orbit potential is nearly the same as that obtained for single nucleons, which differs from the prediction of the theoretical model,^{11,12} according to which a value approximately one-third of the single-nucleon value is to be expected. With the same geometry as that obtained previously, a series of searches starting from $V_{so}=2$ and 3 MeV were conducted, and the best results are shown as dashed curves in Fig. 4. In the case of ${}^9\text{Be}$, the fit obtained with the weaker spin-orbit potential is not as good as the best fit obtained. The fits to the ${}^{10}\text{B}$ and ${}^{11}\text{B}$ data at 2.10 MeV do not distinguish between the two values of the spin-orbit well depth. The 1.75-MeV data for ${}^{11}\text{B}$, on the other hand, are better fitted by the stronger spin-orbit potential, with the weaker one leading to more forward scattering than observed and slightly misplaced extrema. The ${}^{12}\text{C}$ data also exhibit a slight preference for the deeper well.

Because fluctuations in the optical-model parameters for the scattering of 3-15-MeV ${}^3\text{He}$ particles exist,²⁵ the fits obtained at isolated energies may be fortuitous. Continuous, discrete, and form-factor ambiguities in optical-model parameterizations are well known.¹ For example, the data for ${}^{10}\text{B}$, and ${}^{11}\text{B}$ at 2.10 MeV and for ${}^{12}\text{C}$ could be satisfactorily fitted with a four-parameter potential having $r_0=r'_0=1.23$ fm, $a'=0.616$ fm, and searching on the well depths. The resulting potential, however, fails to yield satisfactory fits to the ${}^{11}\text{B}$ data at 1.75 MeV and to the ${}^9\text{Be}$ data. Thus, although the values in Table I cannot be considered a unique representation of the data, they nevertheless supply a parametrization of the elastic scattering in terms of a single set of geometrical quantities which may be further tested by its employment in DWBA reaction calculations.

C. ${}^{19}\text{F}$ and ${}^{20}\text{Ne}$ Nuclei

A similar procedure has been applied to the scattering of tritons from ${}^{19}\text{F}$ and ${}^{20}\text{Ne}$. Because the bombarding

energy and Coulomb barrier are comparable, these data show little structure, and the determination of optical-model parameters is ambiguous. Nevertheless, in some cases certain potentials are incapable of yielding the smooth, concave-upward structure of the data, and ${}^3\text{He}$ scattering from similar nuclei may supply reasonable starting points for calculation.

In Fig. 5 are the results of three attempts to fit the scattering of 2.00-MeV tritons from ${}^{19}\text{F}$. The dotted curve was obtained by employing the geometry obtained in the analysis of the scattering from the p -shell nuclei previously mentioned and searching on the well depths. The result of the calculations is convex upwards in the forward direction, in disagreement with experiment. The dashed curve was obtained by setting the real and imaginary radii of Ref. 7 equal, and then searching on four parameters in order to achieve a best fit.¹⁷ The solid curve, which nearly coincides with the dashed, was obtained by reducing, according to the prescription of Eq. (3), the real radius obtained in an analysis²⁰ of ${}^3\text{He}$ scattering from ${}^{19}\text{F}$, retaining the other geometrical parameters of that work, and searching on the well depths V and W . The two-parameter fit shown is in fact the starting point itself.

The curves shown in Fig. 6 are the results obtained by the preceding method for the scattering of tritons from ${}^{19}\text{F}$ and ${}^{20}\text{Ne}$. It was not possible to fit the rise near 165° in the ${}^{20}\text{Ne}$ cross section, and it was not possible to determine whether this failure is due to the parametrization or to the presence of compound elastic scattering. There was also an attempt to determine the possible effect of the spin-orbit potential, but in the absence of an empirical guide, only the theoretical value of about 2 MeV was considered, with the result that there are no visible differences from the solid curves. Thus, these scatterings provide no information about the effect of the spin-orbit force. The potentials corresponding to the curves of Fig. 6 are shown in Table II, for which remarks similar to those regarding Table I are applicable. In the present case, the imaginary radius is the same as that obtained for ${}^3\text{He}$. However, if it is reduced in accordance with Eq. (3), then the real and imaginary well depths for the 2.0-MeV data for ${}^{19}\text{F}$ become 136 and 16.5 MeV, respectively, while all other parameters shown are unchanged.

Although the applicability of the optical model to the description of low-energy scattering from light nuclei is questionable, it has nevertheless been possible to obtain parameters for a number of nuclei which relate ${}^3\text{He}$ and ${}^3\text{H}$ scattering and which are in qualitative agreement with theoretical expectation.

ACKNOWLEDGMENT

The authors wish to thank Dr. E. H. Auerbach for the use of ABACUS.

²⁵ J. Y. Park, Nucl. Phys. A111, 433 (1968).